Fluid-Mineral Interactions: A Tribute to H. P. Eugster
© The Geochemical Society, Special Publication No. 2, 1990
Editors: R. J. Spencer and I-Ming Chou

Ironstones of mixed sedimentary and hydrothermal origin in the Archean greenstone belt at Bird Lake, Manitoba

ALLAN C. TURNOCK and DAVID L. TRUEMAN*
Department of Geological Sciences, University of Manitoba, Winnipeg R3T 2N2, Canada

Abstract—This paper describes the forms and associations of aluminous ironstones in volcaniclastic comglomerates in a zone of proximal felsic volcanism, and from 14 bulk rock analyses and element correlations we assign Fe, Mn, Mg, Ca, to a chemical precipitate-exhalative origin, Al, Zr, K, Rb, Si, to a clastic felsite origin, alkali losses to hydrothermal leaching, and variable Ti, Cu, Zn, Mo, Co, V, to unexplained diagenesis.

Iron formations of three facies, chert banded silicate, sulfide ironstone, and aluminous ironstones, are found in an area 1 × 2 km of "Algoma-type" association, with clastic sedimentary rocks and felsic volcanics.

The aluminous ironstones contain iron (as FeO) 16 to 47 wt%. They are garnet + cummingtonite + biotite + hornblende as staurolite-grade metamorphic minerals. They occur as (1) beds and lenses 2 to 60 cm thick, 1 to 30 m long, interbedded in conglomerates; (2) matrix in bimodal conglomerates, *i.e.* mafic matrix to felsite fragments. The mafic matrix has a patchy distribution in conglomerates which have felsic fragments and felsic matrix; (3) filling fractures in a dome of QFP (quartz-felspar-porphyry), that has intruded explosively into the floor of the basin, and, (4) veins (rare) that cut across psammitic beds in the area at the flank of the QFP dome. Types 1 and 2 are mixtures of Fe and the debris of the felsic volcanic rocks. Types 3 and 4 are deposition in fractures from hydrothermal solutions; their presence strengthens the theory of hydrothermal origin.

INTRODUCTION

IRON FORMATIONS are widely distributed in the supracrustal greenstone belts of Archean age of the Canadian Shield (GROSS, 1965; GOODWIN, 1973). The chert-banded-oxide-facies is most widespread, but the other facies (sulfide, silicate, carbonate) are found, especially in the proximal volcanic association (SHEGELSKI, 1975; GROSS, 1980). Seeking to characterize the basins of deposition, GROSS (1980) defined "Algoma type" iron formations as those associated with volcanic and detrital rocks, and in the classification of KIMBERLEY (1978) they are type SVOP-IF (shallow-volcanic-platform iron formation). The source of the iron is attributed to the exhalative output of hydrothermal systems that go with volcanic processes (RIDLER, 1971; GOODWIN, 1973; SHEGELSKI, 1975; GROSS, 1980). All iron formations, including the sulfide facies, are exhalative components in the syngenetic theory of origin of stratiform sulfide deposits (RICHARDS, 1960; HUTCHINSON, RIDLER and SUFFEL, 1971; STANTON, 1976; STANTON and VAUGHAN, 1979).

The intent of this paper is to describe an "Algoman" association of iron formations, felsic volcanics, and detrital sediments, and, for the aluminous ironstones, to try to identify the origin of the elements as belonging to an exhalative component and a detrital component. This is done by examining mixing relationships and correlations in the chemical analyses of 14 ironstones and 4 ferruginous shales from an area 0.5 × 1 km of an Archean greenstone belt, at a felsic volcanic center.

Following the generalized nomenclature of KIMBERLEY (1978), "ironstone" is a sedimentary rock which contains Fe > 15 wt.% (=FeO* > 19.3); and "iron formation" is a mappable rock unit composed mostly of ironstone. An ironstone is here called "aluminous" if Al_2O_3 > 4 wt.%, an arbitrary limit based on inspection. (Note: an asterisk (*) following Fe* or FeO* indicates total iron as either element or oxide).

GENERAL GEOLOGY

The Bird River greenstone belt is one of the east–west trending belts of the Archean Superior Province (Fig. 1A). It is infolded into the English River subprovince between the Manigotagan-Ear Falls paragneiss belt and the Winnipeg River batholithic belt (BEAKHOUSE, 1977). BEAKHOUSE (1985) noted only slight differences between the Bird River belt and other greenstone belts of the province, in greater abundance of felsic volcanics and clastic sedimentary rocks in the Bird River belt.

TRUEMAN (1980) has mapped the Bird River belt and discussed the origin of the major rock types and their tectonic history. The supracrustal formations (Fig. 1B) include the Lamprey Falls me-

* *Present address:* 5433 Collingwood St., Vancouver V6N 1S9, Canada.

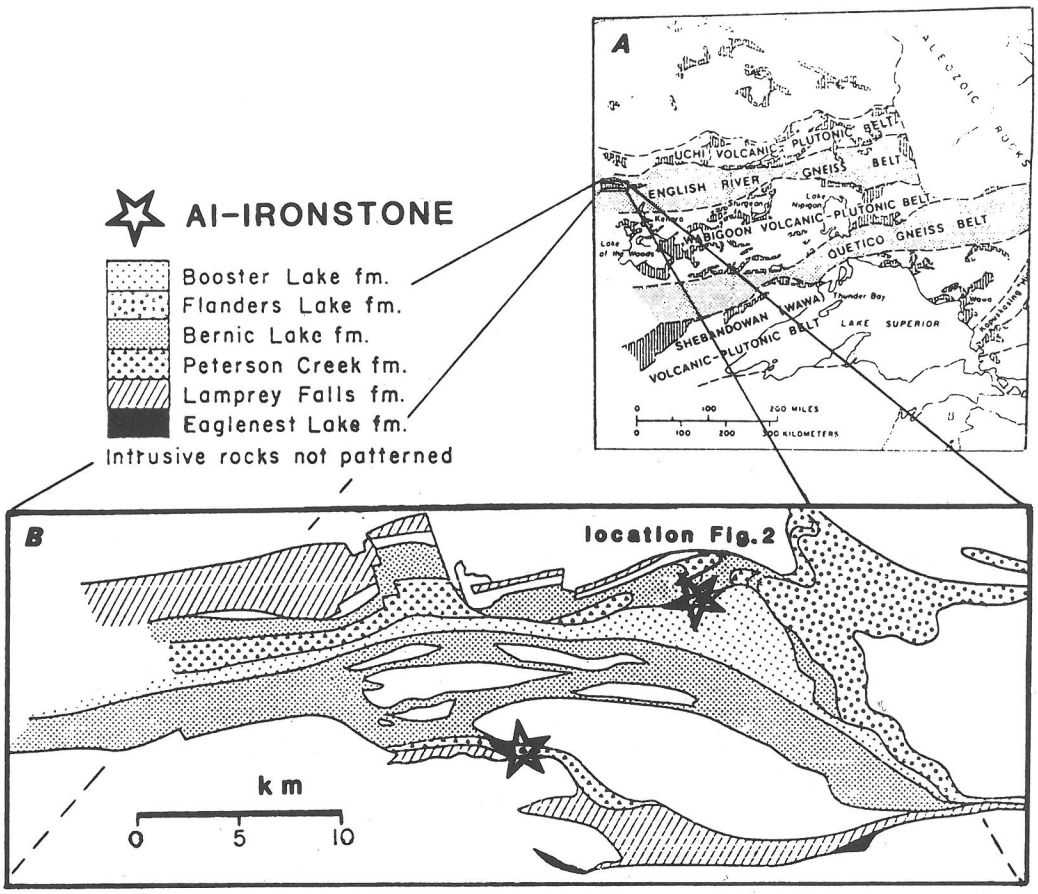

FIG. 1. A. Location of the Bird River Subprovince in the Superior Province of the Precambrian Shield of Canada. B. Map of the lithostratigraphic formations of the Bird River greenstone belt.

tabasalts and the Petersen Creek metarhyolites, a bimodal volcanic suite, and their disposition defines a major east–west synclinorium. The overlying Bernic Lake Formation includes conglomerates, psammites, iron formations, and minor intermediate volcanics. All these formations were deposited subaqueously.

These rocks have been complexly folded and recrystallized at medium grade of metamorphism, and intruded by pre-, syn-, and late-tectonic granitoid stocks and batholiths (TRUEMAN, 1980). There is a dominant east–west S2 foliation. Refolded F1 folds are found in the north-east portion of Fig. 1B, and they are a complication in the study area. It is here assumed that the primary compositions of cation ratios were not changed by metamorphism.

THE BIRD LAKE IRON FORMATIONS

Two localities of abundant iron formations have been found, both are in areas of mostly felsic volcanic rocks and thus mapped as Petersen Creek Fm. (Fig. 1B).

At the Bird Lake locality, three types of iron formations are found interbedded in volcaniclastic conglomerates and psammites, and felsic volcanic rocks (Figs. 2 and 3). They are: (1) Garnet ironstone, found mostly in the lower part of the section (Fig. 3) near the QFP dome, and described below; (2) Sulfide ironstone, traced by magnetometer for 1.5 km as the "SI ANOMALY" across the center of the section, in a bed 7 to 15 m thick (3 cored drill holes, courtesy Tanco Corp.). It is pyrrhotite, with irregular inclusions of garnet-rich aluminous ironstone. (3) CBSIF = chert banded silicate iron formation, found mostly at the top of the section in a bed 50 to 100 m estimated thickness. The outcrop section is thicker, but the individual bands, thickness 1 to 18 cm, are complexly folded in the style called "soft-sediment slump", and this is structural thickening. The silicate bands are mostly por-

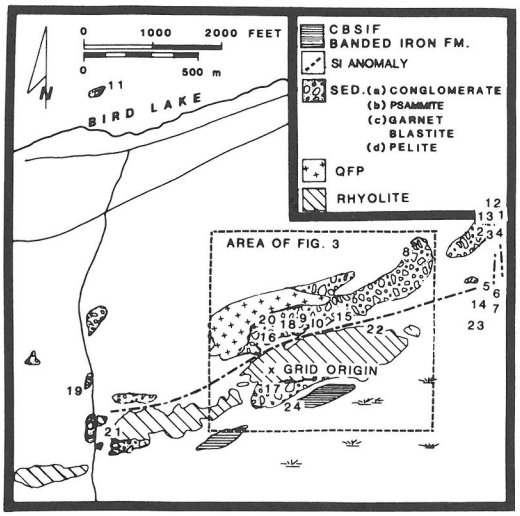

FIG. 2. Area south of Bird Lake, with numbered sample sites. GRID ORIGIN is for sample locations, which are given in Table 1 in feet from origin. CBSIF = chert banded silicate iron formation. SI = sulfide ironstone (anomaly location from magnetometer survey). QFP = quartz feldspar porphyry.

phyroblastic grunerite plus rare actinolite and sulfide, or, hornblende plus cummingtonite. A chemical analysis of a grunerite band is given (Table 1B, #24).

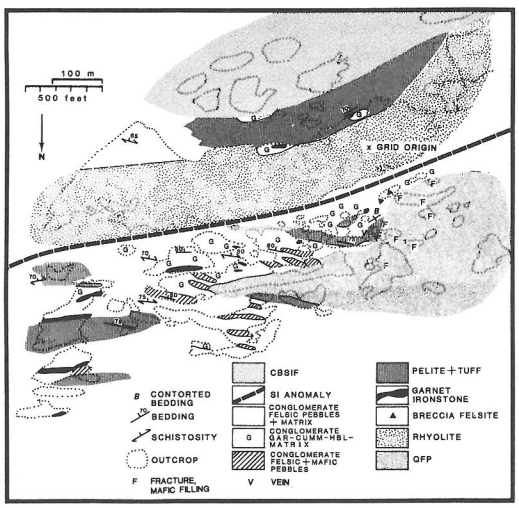

FIG. 3. Detail of the area marked near the center of Fig. 2. CBSIF = chert banded silicate iron formation. SI = sulfide ironstone (anomaly location from magnetometer survey). QFP = quartz feldspar porphyry. GRID ORIGIN is reference 0E, 0N, for locations, distances in feet in text. The map is oriented with north down, section facing up, based on intrusive structures of QFP, and rare graded beds.

Table 1A. List of samples. Analyses in Table 1B

Sample	No.	Location†	Type and reference
1	1–77	3200E, 2280N	ironstone bed
2	1–127	3200E, 2250N	ironstone bed
3	2–201	3540E, 2000N	ironstone bed
4	2–505	3751E, 2000N	ironstone bed
5	3–237	3200E, 1134N	ironstone bed
6	3–267	3200E, 1113N	ironstone bed
7	3–276	3200E, 1107N	ironstone bed
8	2854b	1980E, 1700N	ironstone bed
9	2653d	480E, 600N	ironstone bed
10	2875a	480E, 600N	ironstone bed
11	2844	2700W, 4100N	ironstone bed
12	1–34	3200E, 2325N	ironstone in conglomerate
13	1–45	3200E, 2300N	ironstone in conglomerate
14	3–384	3200E, 1031N	ironstone in conglomerate
15	2877	1100E, 600N	ironstone in conglomerate
16	2845	0E, 500N	ironstone in conglomerate
17	2872a	0E, 245S	ironstone in conglomerate
18	2886a	45W, 610N	ironstone in conglomerate
19	2649b	2720W, 60S	ferruginous pelite
20	2846	0E, 760N	felsite
21	2652c	2400W, 650S	felsite
22	2876	1600E, 600N	felsitic cobble in conglomerate
23	2866	2800E, 700N	schist, graphite + sulfide
24	2874a	190E, 400S	grunerite layer in BIF
25	FeR-1	Bathurst N.B.	BIF, magnetite, Algoma type*
26	FeR-2	Bruce L., Ont.	BIF, magnetite, Algoma type*
27	FeR-3	Temagami, Ont.	BIF, magnetite, Algoma type*
28	FeR-4	Temagami, Ont.	BIF, magnetite, Algoma type*
29	DG-8	Wallace L., Man.#	chloritic layer, magnetite BIF
30	1530b	Snow L., Man.	chloritic altered rock

* Ref. ABBEY *et al.* 1983.
† Shown in Fig. 2, in feet from grid origin.
# From GABOURY 1984.

By association of the iron formations with volcanics and clastic sediments, they are the "Algoma-type" of GROSS (1980). The felsite dome with breccia top, the tabular, stratiform rhyolite, and angular felsite-block conglomerates (Fig. 3), define a "proximal" and explosive volcanic environment. The occurrence of multifacies of iron formations is also a characteristic of proximity to volcanic centers (GROSS, 1980).

The sedimentary rocks are mostly conglomerates, with clast-supported frameworks and angular fragments. Sorting is absent, and bedding can be

Table 1B. Chemical composition of ironstones

	1	2	3	4	5	6	7	8	9	10	11	12	13	14	15
wt.%															
SiO_2	50.67	36.41	38.95	46.52	65.59	45.98	40.96	27.09	49.94	56.62	45.65	38.80	46.16	45.72	54.58
Al_2O_3	9.18	6.85	13.03	8.07	6.60	2.33	0.55	4.84	13.51	9.85	15.20	8.54	8.48	0.72	14.25
Fe_2O_3	5.44	29.69	0.73	9.25	1.82	23.09	0.64	30.19	4.06	8.59	3.86	14.55	4.33	1.83	2.64
FeO	21.88	14.48	34.00	21.92	15.14	13.80	39.62	19.68	22.72	19.24	26.42	25.28	26.28	35.66	16.84
MgO	2.86	2.77	2.46	3.72	2.84	4.46	3.93	5.79	3.01	2.80	2.43	2.86	2.86	4.37	2.78
CaO	2.58	1.00	3.76	4.65	2.34	4.68	5.78	5.83	1.91	1.75	1.99	1.61	4.51	4.09	2.49
Na_2O	0.08	0.15	0.03	0.26	0.02	0.04	0.01	0.16	0.08	0.01	0.29	0.04	0.38	0.00	1.24
K_2O	1.82	0.92	0.12	1.38	2.36	0.63	0.03	0.01	2.36	0.34	0.64	1.68	0.90	0.05	1.14
H_2O^+	2.37	1.78	1.40	1.82	1.44	0.92	1.73	1.30	1.53	2.78	0.91	1.66	1.36	1.94	2.20
CO_2	0.44	0.01	1.41	0.50	0.12	1.00	0.66	0.54	0.54	0.34	0.29	0.18	0.25	0.02	0.35
TiO_2	0.10	0.16	0.61	0.21	0.12	0.17	0.01	0.20	0.41	0.22	0.74	0.37	0.19	0.01	0.55
P_2O_5	0.03	0.36	0.21	0.05	0.03	0.03	0.00	0.02	0.07	0.02	0.02	0.08	0.07	0.01	0.06
MnO	2.35	2.81	2.00	1.80	1.04	2.44	2.17	2.87	1.01	1.54	0.75	2.37	2.21	2.60	0.47
S	0.35	3.49	1.25	0.47	1.03	0.64	6.56	0.04	0.007	0.05	0.124	3.62	2.74	4.72	0.205
ppm															
Zr	82	76	74	70	100	32	9	32	114	94	57	135	140	11	155
Li	24	13	19	19	35	15	7	2	47	6	39	19	12	5	19
Ba	158	169	157	65	—	122	60	119	184	99	160	235	124	64	240
Be	—	—	1	—	<1	2	—	<1	1	1	1	<1	<1	2	1
Co	3	6	42	42	4	3	4	7	41	6	47	25	14	7	17
Cu	18	21	76	73	95	46	31	34	17	101	120	38	37	41	182
Mo	5	6	11	3	3	12	—	3	7	9	7	11	12	<1	—
Ni	3	26	71	75	12	51	30	18	82	13	88	43	29	18	41
Pb	—	—	—	—	—	—	—	—	—	—	—	—	—	—	—
Rb	73	34	10	10	121	36	1	2	98	22	70	32	28	4	41
V	—	29	109	—	107	1	1	24	35	6	183	60	2	—	64
Zn	17	33	55	93	39	53	41	64	124	84	60	93	37	34	118

	16	17	18	19	20	21	22	23	24	25	26	27	28	29	30
wt.%															
SiO_2	61.44	50.70	48.13	58.86	71.90	73.78	75.28	86.29	51.50	16.99	49.03	53.51	50.41	59.93	27.26
Al_2O_3	11.16	11.25	8.78	12.31	13.87	14.30	13.58	4.43	1.04	0.55	5.20	0.03	1.75	15.78	19.76
Fe_2O_3	4.06	4.71	3.07	3.65	1.12	0.85	1.51	2.76	3.82	49.93	22.53	28.65	23.23	2.52	4.82
FeO	12.70	19.32	26.78	12.88	2.74	1.16	0.84	0.62	31.64	23.20	14.85	14.10	15.10	10.96	14.76
MgO	2.77	3.19	3.07	3.33	0.73	0.54	0.51	0.38	3.54	0.24	2.02	0.96	1.39	1.43	18.26
CaO	0.31	4.92	5.02	5.49	2.46	0.46	0.29	0.94	3.17	3.37	2.18	0.89	2.29	3.83	1.51
Na_2O	0.03	1.55	0.13	0.58	4.01	4.96	3.76	0.66	0.02	0.05	0.48	0.03	0.04	1.43	0.11
K_2O	4.31	0.74	0.23	0.78	1.48	2.43	2.88	0.34	0.04	0.01	1.29	0.03	0.26	0.49	0.28
H_2O^+	1.87	1.47	1.69	1.10	0.78	0.81	1.00	0.64	2.55	0.32	0.93	0.25	0.83	3.31	10.36
CO_2	0.25	0.25	0.28	0.16	0.27	0.09	0.11	0.28	1.38	1.38	0.04	1.21	4.88	0.10	0.94
TiO_2	0.24	0.41	0.25	0.52	0.42	0.16	0.14	0.18	0.02	0.03	0.21	0.01	0.07	0.37	0.68
P_2O_5	0.01	0.11	0.06	0.14	0.08	0.02	0.02	0.04	0.02	2.37	0.32	0.07	0.12	0.12	0.03
MnO	0.86	1.16	1.90	0.45	0.18	0.01	0.03	0.23	1.99	0.26	0.12	0.08	0.20	0.20	0.47
S	0.039	0.002	0.015	0.014	0.006	0.004	0.003	0.324	0.06	0.26	0.18	0.02	0.09	0.006	0.481
ppm															
Zr	131	92	74	152	294	213	182	161	3	10	35	—	51	223	171
Li	54	24	5	12	18	21	22	4	<1						46
Ba	136	57	35	31	121	80	90	240	87	1030	229			206	117
Be	<1	1	1	<1	1	<1	1	<1	1						1
Co	17	11	9	27	6	6	8	5	1					4	6
Cu	27	15	18	133	13	15	13	17	12					11	53
Mo	1	4	5	2	6	—	<1	19	3					3	13
Ni	18	39	26	89	10	1	7	3	7					18	2
Pb	—	—	—	—	—	9	6	4	—						34
Rb	231	23	14	19	62	109	111	6	2					15	7
V	11	40	—	56	—	—	—	63	—	95	34	8	10	28	40
Zn	114	61	57	108	32	34	29	10	21					34	2040

Table 1C. Correlation of elements† $r > 0.55$

	Positive		Negative	
	#1–11	#1–30	#1–11	#1–30
Si	Rb, K, Zr, Li	Zr, Na	Fe*, Fe^3, Mn	Fe*, Fe^3
Al	Co, V, Zr, Li, Ba	Zr, Li	Mg, S, Ca	
Fe^3	Mg	P, Ba, Fe*	Fe^2, Si	Si
Fe^2		Mn, Fe*	Fe^3	Zr, Si, Na
Fe*	Mn	Fe^2, Fe^3	Si	Si, Zr, Na
H_2O		Zn, Mg	Ti	
CO_2	Mo			
Ti	Mo, Ni		Mn, H_2O	
P		Ba, Fe^3		
Mn	Fe*	Fe^2	Ti, Si	
Zr	K, Al, Rb, Si, Li, Ba	Al, Na, Si	Ca, Mg, S	Fe^2, Fe*
Rb	K, Li, Si, Ba, Zr	K, Li	Ca, Mg	
K	Rb, Li, Zr, Si	Rb, Li		
Na	Co, V	Zr, Si		Fe^2, Fe*
Li	Rb, K, Al, Ba, V, Zr, Si, Co	Rb, Al, K	Mg, Mn	
Mg	Ca, Fe^3	Zn, H_2O	Zr, Al, Li, Rb	
Ca	Mg		Zr, Ba, Al, Rb	
Ba	Rb, Al, Li, Zr	P, Fe^3, Mo	Ca	
S			Al, Zr	
Co	Ni, Al, V, Zn, Li	Ni		
Cu	V			
Mo	Ti, CO_2	Ba		
Ni	Co, Ti, Zn	Co		
V	Cu, Co, Al, Li			
Zn	Ni, Co	H_2O, Mg		

† SAS 1983 proc corr.
Fe* = total iron.

mapped only by the presence of clasts of mafic volcanic rock in uncommon beds (Fig. 3). These beds are lensoid, mostly 5 × 50 m, rarely 10 × 100. Uncommon psammitic and pelitic beds are lenses less than 100 m in length (Fig. 3). Such sediments are high-energy types, suggesting active faulting. The clasts are volcanic, there is no evidence here for a hinterland of gneissic or granitic rocks. The clasts are mostly felsic volcanic rock, plus mafic in some beds (Fig. 3), plus rare cobbles of ironstone and sandstone.

The environment of deposition can therefore be interpreted to be a lake, fault-bounded, with internal and external felsic volcanoes. The most extensive beds are the sulfide ironstone and the chert banded silicate iron formation. These chemical precipitates must form in the basin in a short time between episodes of debris flows and volcanism, which requires an input of fluid rich in Fe, S and Si. The fluid is theoretically hydrothermal exhalations, from a major system centered on the submarine volcanoes.

GARNET IRONSTONES

The garnet-rich rocks of the Bird Lake area occur in 4 structures, viz: (1) lensoid beds; (2) matrix of conglomerates; (3) filling fractures in QFP; (4) veins. Sample locations are shown in Fig. 2; Fig. 3 is the portion mapped at 1 = 6000.

Type 1, lensoid beds

Lensoid beds of ironstone make up ½–1% of a wedge of clastic sediments beside an intrusive dome (QFP) and below a bed of sulfide ironstone (Fig. 3). The longest and most regular is 0.3 m thick and 20 m long, stratiform in shape and in strike parallel to other sedimentary beds. Several smaller ones, which may be disrupted beds, are lenses or irregular pods, with sizes varying from 1 × 2 m, to 0.2 × 0.2 m. There are also a few small pods in that part of the section above the rhyolite (top of Fig. 3). These ironstones are aluminous, with 10 to 80% garnet, and Al_2O_3 5 to 15% (Table 1, #1–11), except for #6 and 7; they are cummingtonite ironstone (#6) and a cummingtonite-sulfide ironstone (#7) with Al_2O_3 < 4 wt%.

A lens of aluminous ironstone 1 × 5 m, surrounded by cm-scale bedded psammites and conglomerates (Fig. 4A), has 60% garnet and has contents of FeO* (26–27 wt%) and Al_2O_3 (10–14%) (analyses #9 and 10, Table 1). The range in composition of 3 crystals of garnet (#9 in Table 2) are almandine 83 to 90 mol%, spessartine 0 to 7% and zoned, grossularite 1 to 8% with one crystal showing zoning, pyrope 1 to 8% also zoned in one crystal.

Figures 4B + 4C show garnet-rich beds 1 to 4 cm thick, interbedded with psammites. They are <2 m long, and appear to have been contorted and disrupted in a soft-sediment style. The location is on the flank of the QFP dome (the area marked "B" in Fig. 3), and these contortions and differences in strike of the bedding (Fig. 3) is evidence of forcible intrusion of the QFP dome.

Fig. 4D shows a pod of garnetiferous-mafic ironstone 2 × 3 m, with an unusual lobate contact with QFP (the contact not shown is with conglomerate) plus included fragments of QFP. The lobate edge is the flank of the QFP dome (close to "B" in Fig. 3, and the features shown in Figs. 4B and 4C), and is interpreted as evidence of liquid (the QFP magma) being squeezed into ferruginous mud.

One of the smaller pods of garnet ironstone, 0.2 × 0.5 m, is shown in Fig. 4E. The irregular shape could be explained by the disruption of a bed by the debris-flow of the surrounding conglomerates, or slumping after their first deposition on a slope. There is chert in this pod, but this is not typical.

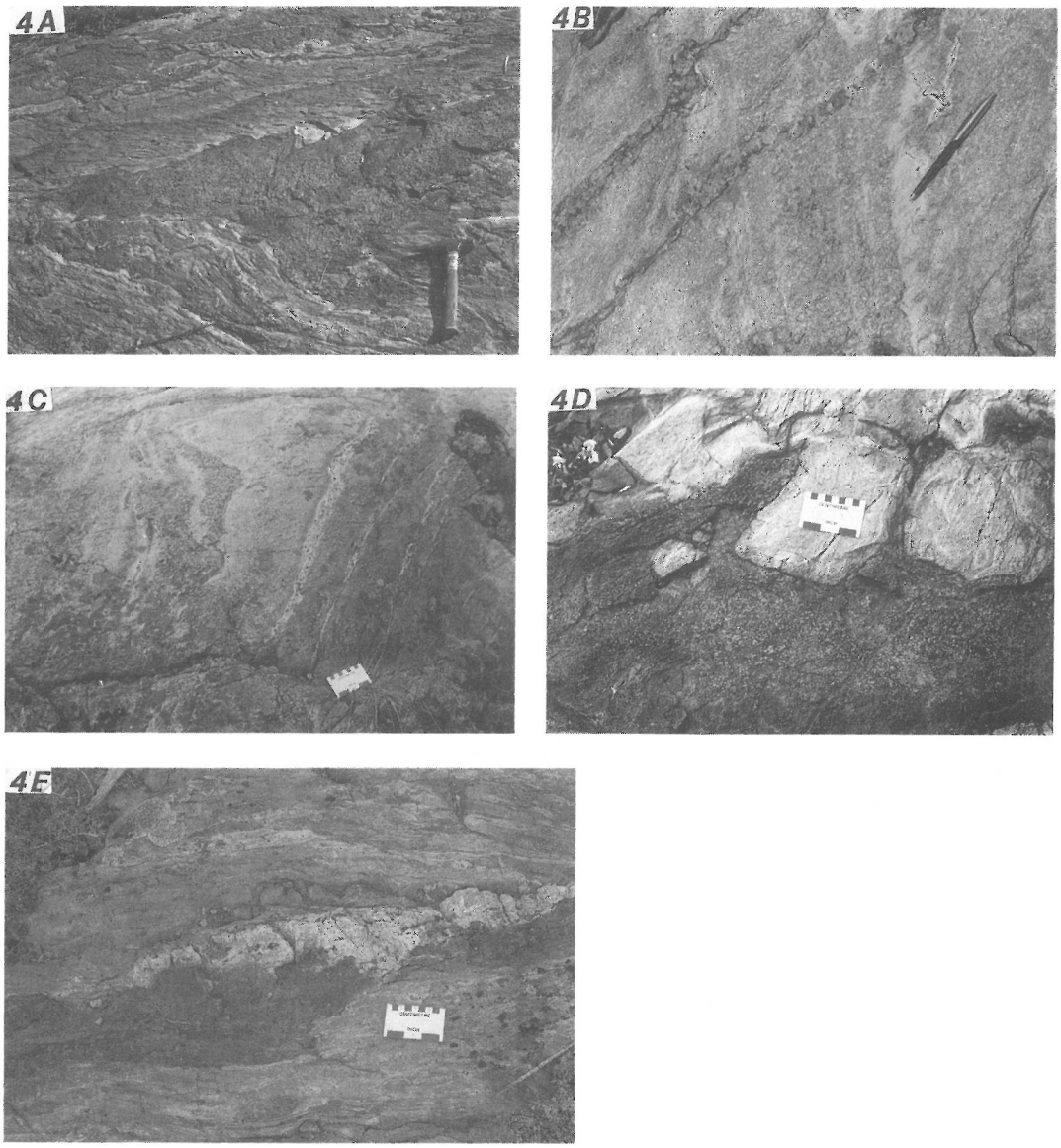

FIG. 4. Ironstones in metasedimentary rocks. Locations are given in feet from "GRID ORIGIN" in Figs. 2 and 3. A: Lens of garnet ironstone in conglomerates and sandstones, 465E, 600N. B: Beds 1 to 5 cm thick of garnet ironstone, pelite and metaconglomerate, cut by veins of garnet type 4, 5E, 560N. C: Beds of garnet ironstone, disrupted; 20W, 580N. D: Pod of garnet ironstone with lobate felsite edge, 35W, 585N. E: Pod of garnet ironstone 0.2 × 0.5 m, with chert edge, 825E, 625N.

Elongation of the felsite clasts, and the ironstone pod, is metamorphic S2.

Smaller pods of garnet ironstone, <0.2 m, are found in the conglomerates, where they may be matrix, pieces of disrupted beds, or pebbles.

Type 2, matrix in conglomerates

The garnetiferous, mafic matrix of some conglomerates is aluminous ironstone (Table 1, #12–18). It is therefore part of a mixed chemical and clastic sedimentary rock, with a bimodal composition (mafic matrix vs. felsic clasts).

These bimodal conglomerates are found in patches of irregular size and shape, in conglomerates and usually close to type 1 lensoid beds of garnetiferous ironstone, at locations marked "G" in Fig. 3. They are not large enough to be mappable, but they make up approximately 1% of the sedimentary pile. The clasts are mostly QFP or rhyolites, the lithologies of the surrounding volcanics. There are

Table 2. Garnet analyses, microprobe*

No.#	Sample	Location	Type	Alm	Spe	Gro	Pyr
1	1–77	3200E	bed	77	17	2	4
		2247N		62	21	15	1
				61	21	16	3
				58	24	17	1
				55	28	18	0
				64	20	15	1
9	2653d	480E	bed	87	3	8	2
		600N		90	1	8	2
				84	6	8	2
				83	6	8	2
				86	4	8	2
				85	5	8	2
				87	3	8	2
9	2653c	480E	bed	84	5	8	3
		600N		88	2	8	3
				89	1	8	3
9	74–79	480E	bed	90	1	2	8
		600N		89	2	5	4
				85	7	7	1
				90	3	6	2
				90	0	3	6
				90	1	1	7
11	2844	2700W	bed	90	2	2	5
		4800N		90	2	2	6
				90	2	2	6
				90	2	2	5
				86	6	5	3
12	1–34	3200E	in conglom-	67	18	12	2
		2276N	erate	44	41	14	0
				45	42	13	0
				60	26	14	0
				77	13	7	3
19	2649c	2520W	pelite	83	6	5	6
				82	7	5	6
				81	8	5	6
				84	5	5	5
—	2654c	100E	pelite	77	18	2	3
		660N		78	16	2	4
				78	16	2	4
				77	17	2	4

* University of Manitoba MAC-5. Beam accelerating voltage 15 kV, at 10 nA. EDS spectra were collected by a Kevex 7000, and corrected by Colby-MagicV program. Analyzed standards: pyrope, grossularite, spessartine, diopside.

The No. refers to bulk chemical analyses in Table 1.

also rare clasts of other types, *i.e.* felsic tuff or sandstone, garnet ironstone, and sulfide, these are intraformational clasts. The primary conglomerates were clast-supported, clast sizes 1 to 300 mm, angular to subrounded; metamorphic flattening has produced minor to severe elongation (Fig. 5A *vs.* Fig. 4A).

The conglomerates which surround them are not bimodal. They are similar in type and shape of clasts, but the matrix of fine-grained quartz and feldspar is felsic and similar in composition to the clasts. These conglomerates also have a clast-supported framework. They are without internal structure, and beds are only rarely outlined by a lens of ironstone or psammite. They are mappable in the lower part of the section (Fig. 3) by the content of clasts of mafic-volcanic rock. These beds are mostly 5 × 20 m, the largest is 20 × 100.

The largest patch of bimodal conglomerate was 5 × 8 m. The smallest was impossible to define, because the host conglomerates include scattered small patches of mafic matrix, sizes in cm and mm, many of which were rounded and are interpreted as intraformational clasts of ironstone. There were no vein structures of garnetiferous material, or continuity of the patches.

The matrix is 5 to 50% garnet, + hornblende, cummingtonite, quartz, biotite. The composition of a garnet (#12 in Table 2) is richer in Mn than the type 1 garnets. The crystal is well-zoned, with contents of spessartine 42 mol% in the core, 13% rim.

Fig. 5A shows a bimodal conglomerate with clast/matrix about 60/40. The clasts are felsite, with continuous size variation from 1 mm to 25 cm. The surface shows mild elongation of the smaller pebbles in metamorphic S2. Fig. 5B shows a similar rock, mafic matrix 35%, in which the clasts are tectonically flattened to 2:1 elongation in S2 (a foliation, strike 90–100°, dip 70–80°S, Fig. 3).

Fig. 5C shows a transition from bimodal conglomerate to brecciated QFP with garnetiferous material filling interstices or fractures. The breccia is at the top of the QFP dome (Fig. 3), and the elongation of the fragments is not tectonic, but due to a primary fracture pattern in the QFP. Fig. 5D is an area adjacent to Fig. 5C, it shows the brecciated QFP with a prominent 15 cm vein of garnet ironstone which contains 25% felsite fragments.

Chemical analyses of mafic matrix were done after cutting or picking out felsite clasts, but clasts smaller than 4 mm were not separated. These compositions (Table 1, analyses #12–18) are similar to those of the lensoid beds (type 1), *i.e.* aluminous ironstones, with two qualifications. Sample #14 is a silicate-sulfide ironstone of cummingtonite and pyrrhotite; this rock type is found in cm-scale lenses in the mafic matrix intermixed with the garnetiferous types. #16 has a content of FeO* (16.3 wt.%) slightly less than the definitive amount for ironstone, and should be called ferruginous pelite.

An hypothesis of origin for these bimodal conglomerates is by the mechanical mixing of felsite

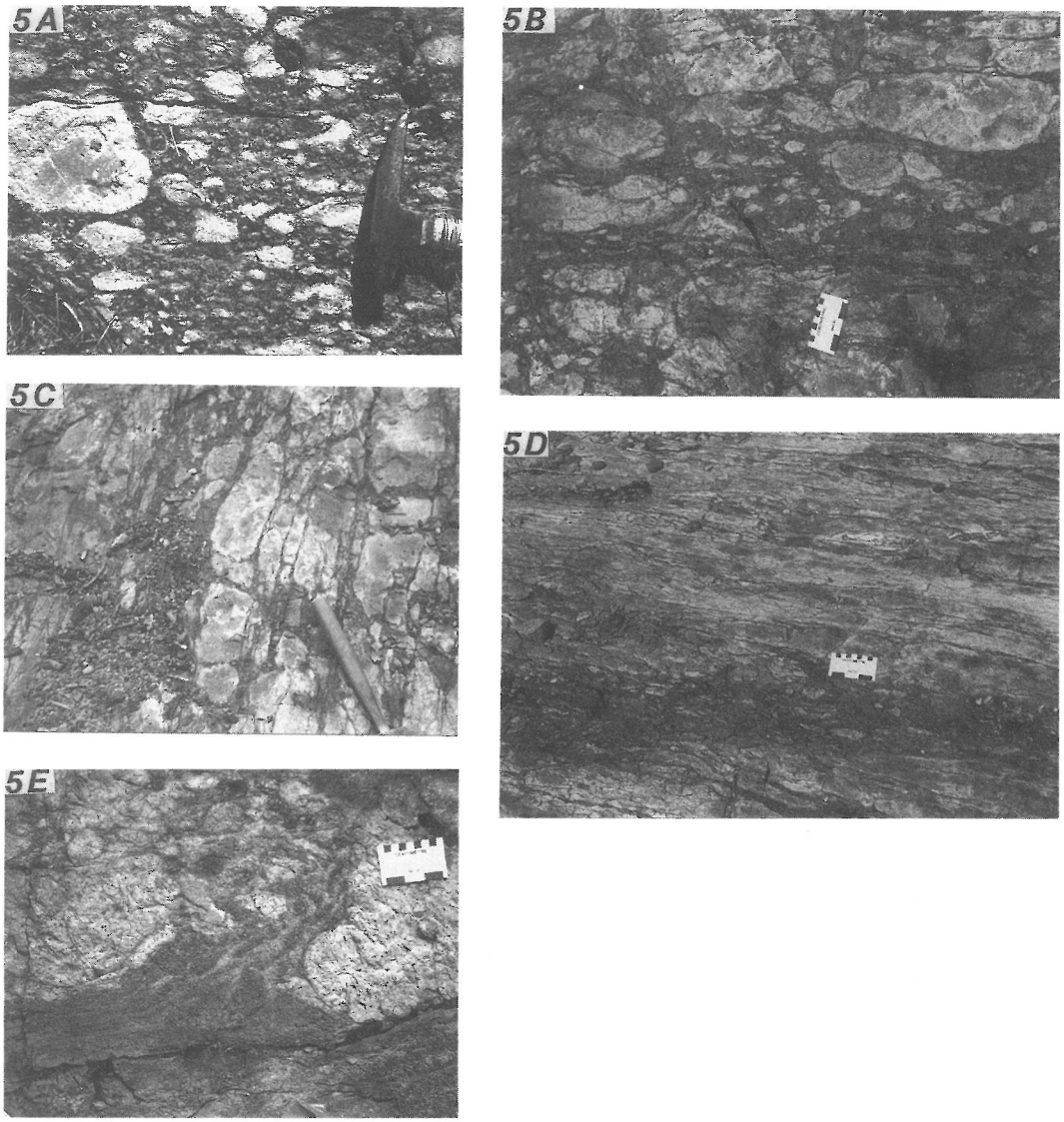

FIG. 5. Ironstone in metaconglomerates and breccias. Locations are given in feet from "GRID ORIGIN" in Figs. 2 and 3. A: Conglomerate, felsic fragments in garnet-mafic matrix, 200E, 450N. B: Same, 100W, 300N. C: brecciated QFP and related conglomerate, both with garnet-mafic matrix, 100W, 300N. D: same, 150W, 300N. E: Flame-like structure of ferruginous pelite bed into felsic conglomerate, 2150W, 815S.

fragments with ferruginous mud. A flame-like structure with swirly mixing lines (Fig. 5E) illustrates the incorporation of mafic mud into a conglomerate. Such a process should be favored by the alternate deposition of a squishy ironstone mud and a conglomerate debris flow. It explains the patchy distribution of the bimodal conglomerate and its association with ironstone lenses and beds.

The origin of bimodal breccias at the top of the QFP dome (Figs. 5C, 5D, 6C) is not known, and may be complex. Ferruginous mud may move down fractures during brecciation, and/or hydrothermal precipitation and alteration may be active.

An origin of the mafic matrix of conglomerates by hydrothermal alteration of the chloritization type is not favored, because the contents of Fe and Ca are too high, and there is no apparent alteration of the fragments. For example, chloritic pipes at Noranda have "major additions of Fe and Mg, and depletions of Ca, Na and Si" (LYDON, 1984). The chlorite alteration pipe at the Anderson Mine has Fe/Mg = 1 (Table 1, #30), versus ratios of 5 to 10

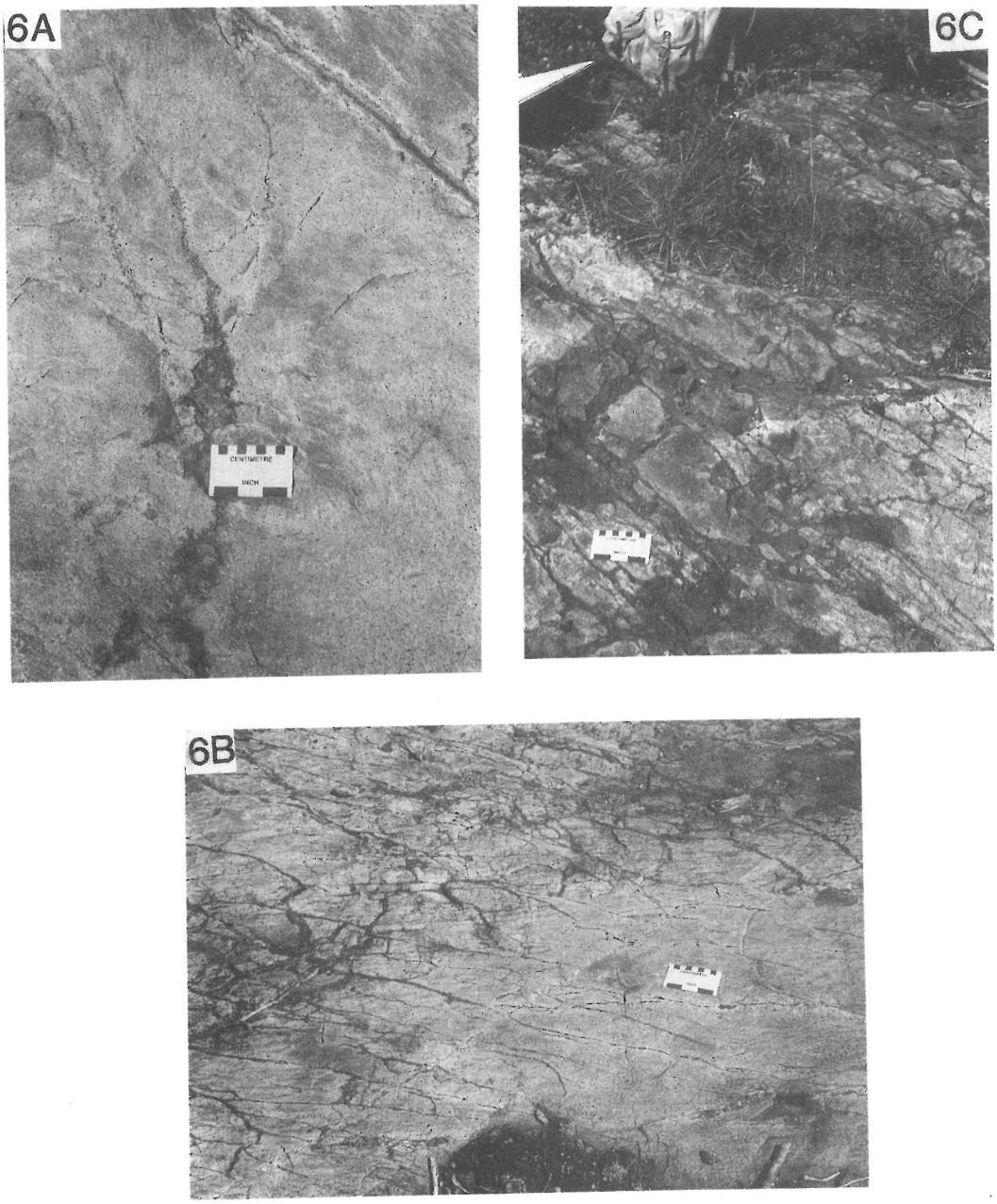

FIG. 6. Discontinuous fractures and brecciation in QFP, filled with aluminous ironstone. A: 400W, 490N. B: 100W, 600N. C: 100W, 350N. Locations are given in feet from "GRID ORIGIN" in Fig. 3.

for samples 12–18. In contrast to the "siderite enrichment zone" in the alteration pipe at the Mattabi mine (FRANKLIN *et al.,* 1975), the bimodal conglomerates at Bird Lake contain twice as much Fe, and a third as much Ti. Also, in "pseudoconglomerates" the clasts are relics of incomplete alteration. For example, the pseudo-clasts at Sunny Corner are described by SECCOMBE *et al.* (1984): "rounded blocks of altered acid volcanic rock, within a limonitic matrix . . . are pervasively silicified and rimmed by chalcedony and limonite." At Bird Lake, there is no appearance in the clasts of veins or rims of silicification or clay alteration. Also, a chemical analysis of a felsic clast (Table 1, #22) is similar in all elements to the felsites of the QFP dome (#20) and the rhyolite (#21); it shows no leaching of alkalis

or additions of the ironstone hydrothermal elements Fe, Mn, Mg and Ca. Also, there are no obvious channels of hydrothermal flow in the conglomerates.

Bimodal conglomerates may form by mixing of felsic lapilli and basaltic sand in a source area, and be transported as lahars (FRANKLIN, 1976). The ironstone matrix of Bird Lake conglomerates is too low in Ti for this origin.

Type 3, fracture filling

Type 3 structures of garnetiferous rocks are fractures in QFP that are filled with mafic material (garnet, hornblende, cummingtonite, biotite, quartz). The fractures are irregular and discontinuous (Fig. 6A, 6B), in the dome of QFP (Fig. 3), or more orthogonal patterns (Fig. 6C, 5C, 5D) found in the breccia felsite on top of the dome. Both include small patches of ironstone-breccia in wider parts of the fractures (Fig. 5D, 6C). These internal breccias have angular fragments, and are not clast-supported framework types.

The origin of the fractures appears to be from the explosive effects of water getting into the QFP magma as the dome intruded seafloor sediments. The infilling of the fractures by iron-rich material is considered to be contemporaneous with the formation of the fractures, because of suspension of fragments in the breccia patches. These veins are the paths of hydrothermal solutions, but the direction of movement is not known.

Type 4, veins in sedimentary rocks

Type 4 structures of garnetiferous rocks are in rare small veins which cut the bedding of metasedimentary rocks. They are found in the flank of the QFP dome (the area around "V" in Fig. 3). They are 1 to 5 cm wide, 0.5 to 2 m long, and not continuous or connected (Fig. 4B). These veins strike 130°–160°; in direction they fan out from the QFP dome. They are older than the regional metamorphism on the basis that they have M2 minerals and S2 structures. They are interpreted to have formed during the intrusion of the QFP dome, and to indicate that the period of hydrothermal iron metasomatism was active before and after the intrusion.

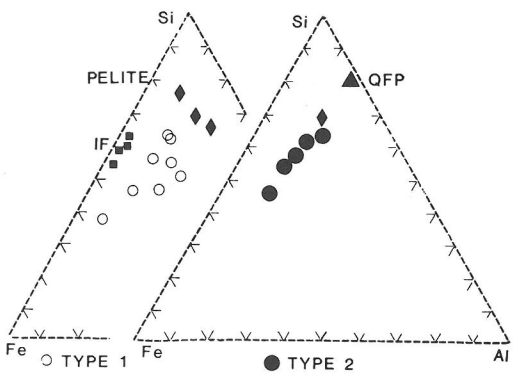

FIG. 7. Atomic ratios Fe/Al/Si, from analyses Table 1. Open circles = aluminous ironstones type 1 (anal. #1–4, 8–11). Closed circles = aluminous ironstones type 2 (anal. #12, 13, 15, 17, 18). Diamonds = PELITE, (anal. #5, 16, 19, 29). Solid triangle = QFP and felsites, 3 analyses (#20, 21, 22). Solid squares = IF iron formation (anal. #6, 7, 14, 24).

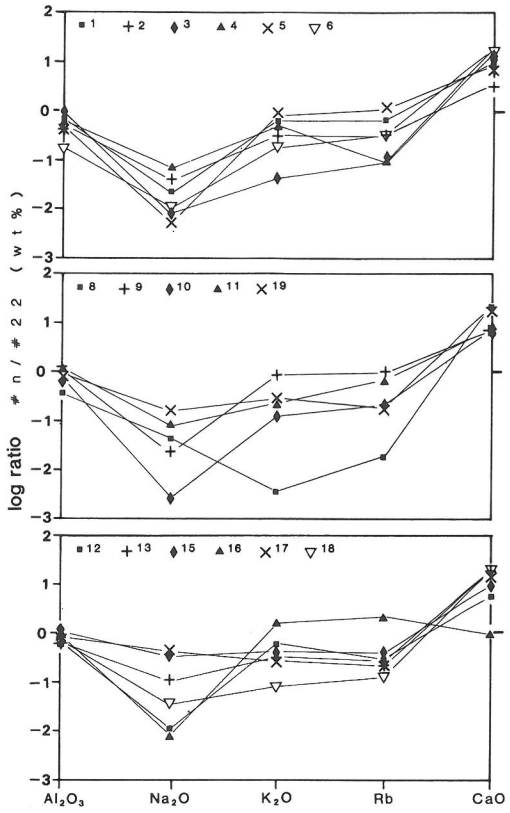

FIG. 8. Comparative contents of alumina, alkalis and lime. Data in wt% (Table 1) normalized against the values for felsite #22. Aluminous ironstones type 1 (#1–4, 8–11) and type 2 (#12–13, 15–18). Pelite (#5). Cummingtonite ironstone (#6).

ALUMINOUS IRONSTONES: ORIGIN AND CHEMICAL VARIATION

JAMES (1966) noted the association of aluminous ironstones with fine-grained clastic rocks, and concluded that they formed by interaction between iron-rich water and clastic particles. EWERS and MORRIS (1981) proposed the settling of felsitic pyroclastic dust into precipitating iron oxides or carbonates to explain the aluminous ironstone layers

in the Brockman IF. These theories may be applied to the rocks at Bird Lake, where the supply of iron-rich water is manifest in the presence of the stratiform iron formations, and where volcaniclastic felsic detritus was abundant.

Compositions in Fe-Al-Si are shown in Fig. 7. There are 8 points (circles) for the lensoid beds (type 1) of aluminous ironstone (Table 1, #'s 1–4 and 8–11), they have a large variation in Fe/Si but only a small variation in Si/Al. For the other analyses in the Type 1 group, #5 had only 16.8% FeO*, so it is plotted as pelite (Fig. 7, diamond symbol); #6 and 7 are cummingtonite-hornblende-pyrrhotite ironstones (Fig. 7, IF squares). The field of type 1 aluminous ironstones is distinct from the low-alumina iron formations (Fig. 7, IF squares, #'s 6, 7, 14, 24), but this may be due to the small number of samples. They also differ from reference oxide iron formations (analyses 25–28, Table 1) in having more Al and Mn, but less P. The type 1 aluminous ironstones and the pelites (#5, 19, 29) have a trend that is interpreted as mixing of exhalative Fe with the Si + Al of the clastic debris of the felsic volcanic rocks.

This mixing trend is similarily defined by the points for the ironstone matrix of conglomerates (Fig. 7, solid dots, analyses #12, 13, 15–18, + pelite diamond #16). The trend is from Fe towards the point QFP (Fig. 7, triangle), which includes 3 analyses of felsites (#'s 20–22). The felsites have Si/Al = 4, and this ratio controls the trend with minor scatter. This trend is not the same as the mixing of Fe and kaolinite (Si/Al = 1) to form chamosite (MAYNARD, 1983 p. 44).

Also, the Fe end-member of the trend, the hydrothermal-exhalative component, is not the non-aluminous ironstones (Fig. 7), even though three of these samples (#6, 7, 14) are patches rich in cummingtonite in garnet-ironstone, and the fourth is a silicate band in CBSIF. They have Si/Fe ratios 6/4, which reflects the dominant cummingtonite now present, and which suggests that the original mineral was greenalite (or its precursar, as discussed by EWERS, 1983). The definition of the Fe end-member may be approached in sample #8, which is high in FeO*, Fe^{+3}, Mg, Ca, Mn, and low in Si, Na, K, Rb, Zr, Li, Co, compared to the other aluminous ironstones. Such an element distribution suggests that it was a precipitate of carbonates and iron hydroxides. Carbonates are common in the type section at Algoma (GOODWIN, 1973), where they are preserved in low-grade metamorphism. The exhalative elements Fe, Mn, Mg, Ca, are inter-correlated (Table 1C), but Ca fails to correlate with Fe. The theory of EWERS and MORRIS (1981) applies, that the addition of pyroclastic dust changes the chemistry of precipitation. The reaction is the hydrolysis of feldspar, which decreases the acidity and promotes the precipitation of carbonates. In the Bird Lake aluminous ironstones the reaction is localized, in view of inclusions of cummingtonite (samples #6, 7, 14) and unaltered clasts in the conglomerates, and therefore more of an "in situ" or diagenetic style, than the non-localized, basin-wide change in chemistry proposed by EWERS and MORRIS (1981) for the Brockman IF.

Correlation of Al, Zr and Ti was used by EWERS and MORRIS (1981) to define the pyroclastic component in the Brockman IF. For the Bird Lake aluminous ironstones, there is a correlation of Al with Zr, also a negative correlation of Al with the exhalative elements Mg, S, Ca (but not with Fe). Ti is a clastic component element also at Mt. Isa (FINLOW-BATES, 1979), and in the aluminous ironstones at Bathurst (TROOP and SCOTT, 1985). Ti correlates with Al in the "Fe shales" in the BIF of greenstone belts in the Yilgarn Block (GOLE, 1981); and in the sulfide ores and iron formations at Broken Hill (STANTON, 1976). Ti is part of the tuff component in the "tuffaceous exhalites" at Redstone (ROBINSON, 1984). At Bird Lake, however, TiO_2 (0.10–0.74 wt.%) has a random variation vs Al in samples 1–11, and cannot be assigned to the detrital component. Ti has a positive correlation with Mo and Ni, and a negative correlation with Mn (Table 1C). This could be explained by movements of Ti, Mo and Ni in a diagenetic process after deposition, or a hydrothermal alteration process in felsite before or during deposition.

Some transition metals in the metalliferous sediments of the area of the East Pacific Rise have been assigned with Fe and Mn to an origin from hydrothermal exhalations. They are Cu, Cr, Ni, Pb (BOSTROM and PETERSON, 1966), Cu, Zn (DYMOND, 1981), and Cu, Zn, Ni, Co, Pb, (BARRETT *et al.* 1987). In the Bird Lake ironstones, however, no correlation is found between the transition elements and the exhalative group Fe, Mn, Mg, Ca. The transition elements correlate with each other, and, for Co and V, with Al, and, for Mo and Ni, with Ti. Their behaviour, like Ti, is complex, and related to hydrothermal alteration of the felsite.

The variability of alkali contents in the Bird Lake ironstones is shown by ratio comparison, normalizing with compositions of the felsic volcanic #22 in Table 1 (Fig. 8). The ratios for Al are slightly less than 1, this is dilution of felsite by the hydrothermal component on the assumption that Al is an inert (stable) element. The ratios for Na are consistently lower, therefore Na is interpreted to have been leached from the felsite detritus. The ratios for K are similar to those of Al, or lower, but not as low

as for Na. Therefore K is interpreted to be variably leached, but resistant to the leaching relative to Na. The behaviour of Rb is similar to that of K (Fig. 8) and they correlate (Table 1C). Leaching of Na and variable leaching of K is typical of alteration zones of hydrothermal systems (MEYER and HEMLEY, 1967), but whether this occurred during precipitation or diagenesis, or whether the felsite was attacked before the detrital stage, is not known. For Ca contents, the ratios to felsite are positive (Fig. 8); it is interpreted as a precipitated element.

CONCLUSIONS

Iron formations of the chert banded silicate, sulfide, and aluminous silicate types formed in proximity to centers of felsite volcanism, interbedded with volcaniclastic tuffs, conglomerates, and breccias. Vein fillings of ironstone in a felsite dome intrusion indicate that hydrothermal systems were active in transporting iron.

Aluminous ironstone formed by the mixture of felsite tuff with exhalative Fe-rich solution and their Si-Fe precipitates on the sea floor, and with Fe-Mn-Mg-Ca precipitates formed on the sea floor and in diagenesis. Mixing was accompanied by hydrothermal leaching of Na, K and Rb from the felsite. Transition metals were not precipitated with Fe.

The aluminous ironstone formed beds which are smaller than 0.3×20 m; possibly they were larger but they were subject to disruption. Rip-up of these beds by volcaniclastic debris flows created conglomerates with felsic cobbles in a matrix of mafic ironstone.

The Bird Lake aluminous ironstones are similar, except for less Cu + Ni, than the "Fe shales" of the Archean Yilgarn Block in Australia (GOLE, 1981). Possibly, higher Cu + Ni contents in the Yilgarn may result from a source area rich in ultramafic rocks.

The average contents of the Bird Lake aluminous ironstones are similar in Al, Si, Fe, Mg, Na, Ti, Mn, S, Zr, Ba, Cu, and V to, greater in Ca and K than, and lower in P, Co, Ni, and Zn than, the average Algoma silicate IF of the Superior Province of the Canadian Shield (as compiled by GROSS and MCLEOD, 1980). In each of the "similar", "greater", and "lower" groups, there are elements that are assigned to the exhalative component (Fe, Mn, Mg, Ca, P?, S?), the detrital felsite component (Al, Zr, Si, K, Rb, Ba?), and the leached or fixed in felsite elements (Na, K, Rb, Co, V, Ti, Mo, Ni, Cu?, Zn?). Considering the known variability of composition of hydrothermal systems and their deposits, and the complexity of the processes interpreted for the origin of these aluminous ironstones, the clustering of the "similar" elements is remarkable. It indicates that there are constraits on the composition of hydrothermal solutions and their deposits. There is some uniformity of host rocks, which are the igneous types of the Archean mafic-felsic cycle, and their clastic derivatives. Felsic volcanism may be a dominant factor in several ways, such as source of heat and pyroclastic debris, and source of hydrothermal solutions rich in Fe and HCl (WHITNEY *et al.* 1985).

The environment of deposition is interpreted to have been an aqueous basin, with explosive felsic volcanoes in and around it, and active hydrothermal systems and fault scarps. Beds of chert banded silicate iron formation, and sulfide ironstone, precipitated during quiet periods, and aluminous ironstones during periods of volcanic activity. A similar model of origin was proposed for the Helen Iron Formation (GOODWIN *et al.,* 1985). The hydrothermal systems, to carry abundant iron, would be acid and reducing (EWERS, 1983; WHITNEY *et al.* 1985). Aluminous ironstones would form diagenetically and by precipitation, where the exhaled hydrothermal solutions cool, mix, and react with felsite detritus.

The Bird Lake occurrences strengthen the genetic linkage between iron formations and igneous activity, but the source of iron is not obvious. STANTON (1985) has suggested that it should be sought in the igneous processes that produce felsic magma, and a mechanism for the concentration and transportation of iron in felsic rocks and magma is given by WHITNEY *et al.* (1985).

Acknowledgements—Allan Turnock acknowledges the debt owed to Hans Eugster for his teaching of geochemistry in 1957. The Geological Survey of Canada provided a grant for chemical analyses and some of the field work. We thank Drs. G. A. Gross and C. R. McLeod for encouragement and the supply of rock standards for chemical analysis, and G. A. Gross, N. M. Halden, J. J. Hemley, I-Ming Chou, and Wayne Nesbitt for reviews.

REFERENCES

ABBEY S., MCLEOD C. R. and LIANG-GUO (1983) Four Canadian iron-formation samples prepared for use as reference materials. Geol. Survey Can. Paper 83-19.

BARRETT T. J., TAYLOR P. N. and LUGOWSKI J. (1987) Metalliferous sediments from DSPD leg 92: the East Pacific Rise transect. *Geochim. Cosmochim. Acta* **51,** 2241–2253.

BEAKHOUSE G. P. (1977) A subdivision of the western English River Subprovince. *Can. J. Earth Sci.* **14,** 1481–1489.

BEAKHOUSE G. P. (1985) The relationship of supracrustal sequences to a basement complex in the western English River Subprovince. In *Evolution of Archean Supracrustal Sequences,* (eds., L. D. AYRES, P. C. THURSTON, K. D. CARD and W. WEBER), Special Paper 22, pp. 169–178. Geol. Assoc. Can.

BOSTROM K. and PETERSON M. N. A. (1966) Precipitates from hydrothermal exhalations on the East Pacific Rise. *Econ. Geol.* **61,** 1258–1265.

CLIFFORD P. M. (1986) Petrological and structural evolution of the rocks in the vicinity of Killarney, Ontario. Geol. Surv. Can. Paper 86 1B, 147–155.

DYMOND J. (1981) Geochemistry of Nazca plate surface sediments: An evaluation of hydrothermal, biogenic, detrital, and hydrogenous sources. *Geol. Soc. Amer. Memoir 154,* 133–154.

EDWARDS G. R. (1983) Geology of the Bethune Lake area. Ontario Geol. Surv. Report 201.

EWERS W. E. (1983) Chemical factors in the deposition and diagenesis of banded iron formation. In: *Iron Formation Facts and Problems.* (eds., A. F. TRENDALL and R. C. MORRIS) pp. 491–512 Elsevier.

EWERS W. E. and MORRIS R. C. (1981) Studies of the Dales George member of the Brockman Iron Formation, Western Australia. *Econ. Geol.* **76,** 1929–1953.

FINLOW-BATES T. (1979) Chemical mobilities in a submarine exhalative hydrothermal system. *Chem. Geol.* **27,** 65–83.

FRANKLIN J. M. (1976) Role of laharic breccias in genesis of volcanogenic massive sulfide deposits. Geol. Surv. Can. Paper 76-1A, 293–300.

FRANKLIN J. M., KASARDA J. and POULSEN K. H. (1975) Petrology and chemistry of the alteration zone of the Mattabi massive sulfide deposit. *Econ. Geol.* **70,** 63–79.

GABOURY D. (1984) A petrologic study of an Archean banded iron formation, Wallace Lake, Manitoba. Unpublished B.Sc. thesis, Geological Sci., University of Manitoba.

GOLE M. J. (1981) Archean banded iron-formations, Yilgarn Block, Western Australia. *Econ. Geol.* **56,** 897–915.

GOODWIN A. M. (1961) Some aspects of Archean structures and mineralization. *Econ. Geol.* **56,** 897–915.

GOODWIN A. M. (1973) Archean iron-formations and tectonic basins of the Canadian Shield. *Econ. Geol.* **68,** 915–933.

GOODWIN A. M., THODE H. G., CHOU C.-L. and KARKHANSIS S. N. (1985) Chemostratigraphy and origin of the late Archean siderite-pyrite rich Helen Iron Formation, Micipicoten belt, Canada. *Can. J. Earth Sci.* **22,** 72–84.

GROSS G. A. (1965) Geology of iron deposits in Canada. I. General geology and evaluation of iron deposits. Geol. Surv. Can. Econ. Geol. Rept. 22.

GROSS G. A. (1980) A classification of iron deposits based on depositional environments. *Can. Mineral.* **18,** 223–229.

GROSS G. A. and MCLEOD C. R. (1980) A preliminary assessment of the chemical composition of iron formations in Canada. *Can. Mineral.* **18,** 223–230.

HUTCHINSON R. W., RIDLER R. H. and SUFFEL G. G. (1971) Metallogenic relationships in the Abitibi belt, Canada: a model for Archean metallogeny. *Bull. Can. Inst. Min. Metall.* **64**(No. 708), 48–57.

JAMES H. L. (1966) Chemistry of the iron-rich sedimentary rocks. U. S. Geol. Surv. Prof. Paper 440-W.

KIMBERELY M. M. (1978) Paleoenvironmental classification of iron formations. *Econ. Geol.* **73,** 1796–1817.

LYDON J. W. (1984) Ore deposit models 8. Volcanogenic massive sulfide deposits Part 1: A descriptive model. *Geosci. Can.* **11,** 195–202.

MAYNARD J. B. (1983) *Geochemistry of Sedimentary Ore Deposits.* Springer-Verlag.

MEYER C. and HEMLEY J. J. (1967) Wall rock alteration. In *Geochemistry of Hydrothermal Ore Deposits.* (ed., H. L. BARNES) pp. 166–235. Holt, Rinehart & Winston.

RICHARDS S. M. (1960) The banded iron formations at Broken Hill, Australia, and their relationship to the lead-zinc orebodies. *Econ. Geol.* **61,** 72–96 and 257–294.

RIDLER R. H. (1971) Analysis of Archean Volcanic Basins in the Canadian Shield using the exhalite concept. *Bull. Can. Inst. Min. Metall.* **64**(No. 714), 20.

ROBINSON D. J. (1984) Silicate facies iron-formation and strata-bound alteration: tuffaceous exhalites derived by mixing: evidence from Mn-garnet stilpnomelane rocks at Redstone, Timmins, Ontario. *Econ. Geol.* **79,** 1796–1815.

SECCOMBE P. K., LAU J. L., LEA J. F. and OFFLER R. (1984) Geology and ore genesis of Ag-Pb-Zn-Cu sulfide deposits, Sunny Corner, N.S.W. *Proc. Australian Inst. Min. Metall.* **289,** 51–57.

SHEGELSKI R. J. (1975) Geology and geochemistry of iron formations and their host rocks in the Savant Lake - Sturgeon Lake greenstone belts. In *Geotraverse Workshop 1975.* (ed., A. M. GOODWIN) Paper 34. University of Toronto.

SHEGELSKI R. J. (1976) The geology and geochemistry of Archean iron formations and their relations to reconstructed terrains in the Sturgeon Lake and Savant Lake greenstone belts. In *Geotraverse Conference 1976.* (ed., A. M. GOODWIN) pp. 29-1 to 29-22 University of Toronto.

STANTON R. L. (1960) General features of the conformable "pyritic" orebodies. *Trans. Can. Inst. Min. Metall.* **63,** 22–36.

STANTON R. L. (1976) Petrochemical studies of the ore environment at Broken Hill N.S.W. 3-banded iron formations and sulfide orebodies: contitutional and genetic ties. *Trans. Inst. Mining Metall. (Sect. B)* **85,** 132–142.

STANTON R. L. (1985) Stratiform ores and geological processes. *Proc. Roy. Soc. New South Wales* **118,** 77–100.

STANTON R. L. and VAUGHAN J. P. (1976) Facies of ore formation: a preliminary account of the Pegmont deposit as an example of potential relations between small iron formations and stratiform sulfide ores. *Proc. Australasian Inst. Min. Metall.* **270,** 25–37.

TROOP D. G. and SCOTT S. D. (1985) Banded iron formation and sea floor hydrothermal sediments: an Ordivician analog from New Brunswick, Canada. (abstr.). *Geol. Assoc. Can./Mineral. Assoc. Can., Program with Abstracts* **10,** A64.

TRUEMAN D. L. (1980) Structure, stratigraphy and metamorphic petrology of the Archean greenstone belt at Bird River, Manitoba. Unpubl. Ph.D. thesis, University of Manitoba.

WHITNEY J. A., HEMLEY J. J. and SIMON F. O. (1985) The concentration of iron in chloride solutions equilibrated with granitic compositions: the sulfur-free system. *Econ. Geol.* **80,** 444–460.